On Stress-Relaxing Solids:

Part III. Simple Harmonic Deformation

SAUL VELA, J. W. KALB, and A. G. FREDRICKSON

University of Minnesota, Minneapolis, Minnesota

The viscoelasticity of a number of polymer solutions was studied by subjecting the solutions to simple harmonic displacements in a pipe. Both water-based and organic-based solutions were used. Results were analyzed in terms of a modification of the operator equation of linear viscoelasticity. A three-constant model used earlier was found to correlate most of the data. Further experiments to verify the model are suggested.

In previous papers (*4, 7*), a quasilinear hereditary constitutive equation for incompressible materials exhibiting stress relaxation has been derived, and some properties of this equation have been discussed. The equation is

$$S^{ij}(\mathbf{x},t) = -p(\mathbf{x},t)\,g^{ij}(\mathbf{x}) + 2\int_{-\infty}^{t}\psi(t-t')\frac{\partial x^i}{\partial X^m}\frac{\partial x^j}{\partial X^n}\overset{*}{e}^{mn}(\mathbf{X},t')dt' \quad (1)$$

This equation and those derived from it are intended to be valid for very small strain rates only; this should be borne in mind in what follows. An experimental method for determining the relaxation function is the principal topic of this paper.

PERTINENT LITERATURE

It has been shown (*4*) that the relaxation function of materials described by Equation (1) cannot be determined by steady, laminar shear flow experiments alone. In such experiments, one can determine the viscosity η and a normal stress coefficient Θ. The viscosity is related to $\psi(t)$ by

$$\eta = \int_0^t \psi(t)dt \quad (2)$$

and the normal stress coefficient is related to $\psi(t)$ by

$$\Theta = \int_0^t t\psi(t)dt \quad (3)$$

so that steady, laminar shear flow experiments can yield at most the integral and the first moment of the relaxation function.

Kapoor et al. (*7*) have shown how recoil experiments could be used, in principle, to check the applicability of a given relaxation function. This method is not suitable for actual determination of $\psi(t)$, however, for two reasons: initial conditions necessary to keep solutions of the associated boundary value problem simple are difficult to attain experimentally, and solutions of the associated boundary value problem are Fourier-Bessel series so that the computational problem is extremely difficult.

Oldroyd (*9*) suggested and analyzed an experiment whereby the properties of viscoelastic materials could be determined, at least for small rates of strain. This experiment utilized a simple harmonic deformation in a concentric cylinder apparatus. Subsequently, apparatus was constructed and utilized by Oldroyd and his co-workers (*10, 11, 12*) to determine properties of various polymer solutions. Analysis was confined to a certain kind of viscoelastic material; the constitutive equation of this idealized material is tantamount to Equation (1), with the relaxation function given by

$$\psi(t) = \frac{\eta}{\lambda_o}\left[\left(1-\frac{\mu_o}{\lambda_o}\right)e^{-t/\lambda_o} + \mu_o\delta(t)\right] \quad (4)$$

In a later paper, Walters (*14*) has analyzed the experimental results cited above in terms of a somewhat different relaxation function, which also gave a good fit of the data.

The foregoing papers on simple harmonic deformation are subject to criticism on two grounds. First, one can determine two quantities (an amplitude ratio and a phase difference) from the experiment, but only one of them (the amplitude ratio) was fitted to equations derived. If the model is correct, both quantities must fit. Walters (*14*) showed how failure to consider both experimental quantities reduces the sensitivity of the method; he showed that two materials yielding the same amplitude-frequency relation could have quite different phase difference-frequency relations. Second, the primary experimental relation (amplitude-frequency) from which conclusions were drawn exhibits a form which is rather insensitive to the nature of the material being tested. Thus, the experimental system has a natural frequency (when no fluid is in the apparatus, it is a simple torsion pendulum), and amplitude ratio-frequency plots for both elastic and inelastic materials exhibit a maximum near the natural frequency.

From these considerations, it is clear that some alternate method for the determination of the relaxation function is needed. On the one hand, the method should be such that boundary and initial conditions can be attained exactly; it should not be necessary to make approximations such as neglect of inertial terms in the equation of motion, and the form of the solution of the mathematical problem should be simple enough to make computations reasonable. On the other hand, the method should be quite sensitive to the nature of the material, and all data taken should fit the model used.

The authors' candidate for the required method is a system suggested by Broer (*2*) involving oscillatory deformations of material contained in a long pipe of circular cross section. Oscillations are produced by imposition of a sinusoidally varying pressure difference across the ends of the tube. As will be shown, this system meets very satisfactorily the requirements listed above.

Various analyses of the system chosen may be found in the literature. Broer (*2*) gives a correct solution for a Maxwell fluid, though his starting constitutive equation is

Saul Vela is with the Jersey Production Research Company, Houston, Texas.

incorrect [because he used a material derivative, rather than a convected derivative (8)]. The periodic solution of the problem for materials with an arbitrary relaxation function is given by Fredrickson (5); this solution is in terms of the speed of deformation, as are all previous works.

It should be noted that other studies of simple harmonic deformations of viscoelastic deformations have appeared in the literature; a resume is given by Ferry (3). The experimental method reported in this paper has the advantage that local deformations are directly observed (and can be measured, though full use of this was not made in the present study); this is not the case in the sample harmonic deformation experiments described by Ferry.

THEORY

For fluids contained in a long pipe and at rest prior to time $t = 0$, one assumes that the relation between current coordinates and material coordinates in the deformation subsequent to $t = 0$ is

$$r \equiv x^1 = X^1$$
$$\theta \equiv x^2 = X^2$$
$$z \equiv x^3 = X^3 + \int_{t'}^{t} u(X^1, \tau)\, d\tau \qquad (5)$$

where $u(r, t)$ is the axial speed of deformation. One can partially define an axial displacement δ by

$$\frac{\partial \delta(r,t)}{\partial t} = u(r,t) \qquad (6)$$

The definition is completed by specifying a reference configuration. It is convenient to formulate the problem in terms of displacements rather than speed, since the former can be determined directly by the experimental technique described below.

One can now use the method on pp. 139-144 of Fredrickson (5) to show that the displacement is described by the set of equations below, when deformation is driven by a periodic pressure gradient $Re(Pe^{i\omega t})$ applied at $t = 0$:

$$\rho \frac{\partial^2 \delta(r,t)}{\partial t^2} = Pe^{i\omega t} + \frac{1}{r}\frac{\partial}{\partial r}\left[r \frac{\partial}{\partial r} \int_0^t \psi(t-t') \frac{\partial \delta(r,t')}{dt'} dt' \right] \qquad (7)$$

$$\delta(R,t) = 0 \qquad (8)$$

$$\frac{\partial \delta(0,t)}{\partial r} = 0 \qquad (9)$$

$$\delta(r,0) = \text{some arbitrary function of } r \qquad (10)$$

$$\frac{\partial \delta(r,0)}{\partial t} = 0 \qquad (11)$$

Vela (13) has shown that the periodic solution of these equations is

$$\delta(r,t) = Re\left\{ \frac{Pe^{i\omega t}}{\rho\omega^2} \left[\frac{J_0(\alpha r)}{J_0(\alpha R)} - 1 \right] \right\} \qquad (12)$$

in which

$$\alpha^2 \equiv -\frac{\rho i\omega}{\Psi(\omega)} \qquad (13)$$

and Ψ (a complex quantity) is the Fourier transform of the relaxation function:

$$\Psi(\omega) = \int_0^\infty e^{i\omega t}\, \psi(t)\, dt \qquad (14)$$

One sees that computations with this solution require operations on Bessel functions (but not Fourier-Bessel series as in the recoil experiment) of complex argument. This is not a serious obstacle now that high-speed digital computers are generally available.

In what follows, consider deformation at the pipe center line ($r = 0$) only. Put

$$\delta(0,t) = \Delta\, Re\,\{e^{i(\omega t - \phi)}\} \qquad (15)$$

Both Δ and ϕ are functions of frequency, of course.

From Equation (12), it follows that

$$Re\left[\frac{1}{J_0(\alpha R)}\right] = 1 + \frac{\rho\omega^2}{P}\Delta\cos\phi \qquad (16)$$

$$Im\left[\frac{1}{J_0(\alpha R)}\right] = -\frac{\rho\omega^2}{P}\Delta\sin\phi \qquad (17)$$

Hence, if one has measured values of Δ and ϕ for given ω, P, and ρ, the right-hand sides of Equations (16) and (17) may be calculated. One can then solve for the real and imaginary parts of αR on the computer; details of the program are described by Vela (13). Finally, these may be substituted into Equation (13) and the real and imaginary parts of $\Psi(\omega)$ calculated. However, the authors choose instead to compute quantities $\gamma(\omega)$ and $\zeta(\omega)$, defined by

$$\Psi(\omega) = \gamma(\omega) - i\zeta(\omega) \qquad (18)$$

since now $\gamma(\omega)$ and $\zeta(\omega)$ are identical to the quantities η' and η'', respectively, used by Williams and Bird (15) in their study of simple harmonic deformations.

In this way, one arrives at numerical values of the Fourier transform of the relaxation function over a limited range of frequencies. Unfortunately, it is not possible to use these data to obtain the relaxation function without approximation, so a different procedure is resorted to.

In linear viscoelasticity theory, the so-called *operator equation* is held to be the most general constitutive equation [see, for example, Alfrey and Gurnee (1)]. For cases in which the material being studied is at rest for all times prior to $t = 0$, Fredrickson has shown [(5), pp. 125-128] that the operator equation is tantamount to Equation (1), with a relaxation function having Fourier transform

$$\Psi(\omega) = \int_0^\infty e^{i\omega t}\, \psi(t)\, dt = \eta \frac{1 + \mu_0 i\omega - \mu_1\omega^2 - \mu_2 i\omega^3 + \cdots}{1 + \lambda_0 i\omega - \lambda_1\omega^2 - \lambda_2 i\omega^3 + \cdots} \qquad (19)$$

where η is the steady state viscosity, and $\mu_0, \mu_1, \mu_2, \ldots, \lambda_0, \lambda_1, \lambda_2, \ldots$ are properties of the material.

The suggested procedure is to truncate the series in Equation (19) at some selected number of constants and then to fit data to the resulting expressions for $\gamma(\omega)$ and $\zeta(\omega)$. This procedure is somewhat more general than that developed by Oldroyd (9); in his procedure, the number of constants was arbitrarily fixed at three (η, λ_0, and μ_0) beforehand.

Finally, the following limits established by Vela (13) will be useful in the analysis of experimental data:

$$\lim_{\omega\to 0} \frac{4\,\eta\omega\Delta}{R^2 P} = 1 \qquad (20)$$

$$\lim_{\omega\to 0} \lambda(\omega) = \eta \qquad (21)$$

$$\lim_{\omega\to 0} \zeta(\omega) = 0 \qquad (22)$$

Equations (21) and (22) follow directly from Equation

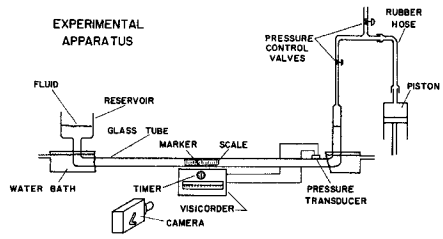

Fig. 1. Schematic diagram of equipment.

(19); Equation (20) can be derived from Equation (12) by expanding the Bessel function $J_o(\alpha R)$ in a power series.

EXPERIMENTAL

Apparatus

Figure 1 is a schematic diagram of the experimental apparatus. The fluid to be studied was contained in the reservoir and the glass tube. Motion of the fluid was driven by a sinusoidal pressure generated in the piston and cylinder assembly. The purpose of the reservoir was simply to supply a constant pressure sink (atmospheric). The objective of the experiment was to measure the deformation in the fluid as a function of time and frequency of pulsation, for a number of selected materials. The effect of amplitude of deformation was also to be studied.

The horizontal glass tube test section had an inside diameter of 2.54 cm. The tube was mounted in a plastic trough through which constant temperature water circulated. At one end, the tube was connected to the glass reservoir; at the other end, it was connected to the pressure source. Connections were made by rubber hoses; these served to damp extraneous vibrations.

The reservoir was a glass vessel 5 in. high and 5½ in. I.D. The outlet to the glass tube had an inside diameter of 1-9/16 in. The reservoir was open to the atmosphere, of course.

At the opposite end of the tube, a compensated pressure transducer, operating on an excitation of 7 v., was inserted in the connection between the glass tube and the pressure source. Distance from the transducer to the bend leading into the reservoir at the other end of the glass tube was 154 cm. This distance was used in computation of pressure gradients. Thus, end effects due to the bend and the reservoir were assumed to be negligible.

Output of the pressure transducer was sent to a preamplifier and was then indicated and recorded on a Visicorder oscillograph. The instantaneous pressure gradient was obtained by dividing the reading of the Visicorder by the length of the apparatus (154 cm., as noted above) and multiplying the result by an appropriate calibration factor. This was determined under static conditions with air pressure and a mercury manometer. The transducer had to be calibrated for each experiment for all attenuations of the preamplifier. Response was found to be linear.

Deformations were followed with the method developed by Kapoor (*6, 7*). At the middle of the glass tube, a 1-mm. hole

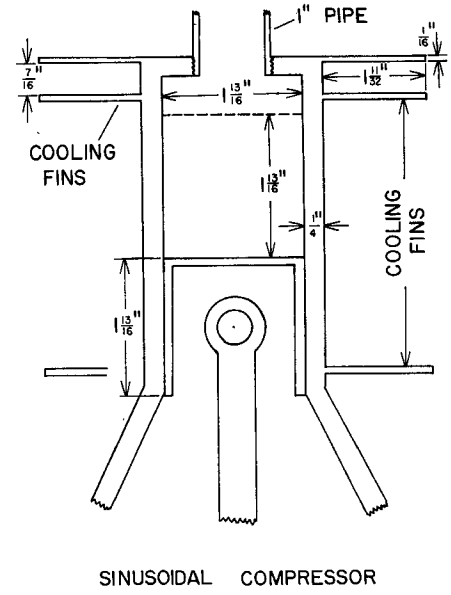

Fig. 2. The piston and cylinder assembly.

was made in the wall with a dentist's drill. A syringe was fitted in an old microscope tube so that it could be moved in the vertical plane in a straight line by the rack and pinion assembly of the microscope. A hypodermic needle was used with the syringe. The syringe was filled with a slurry of carbon particles in the fluid to be tested. The marker was produced by inserting the needle through the hole in the tube all the way to the bottom. Slurry was injected as the needle was removed. Thus, a clearly visible black marker was left. Except with rather thin fluids, this marker had little tendency to disintegrate in the time of an experimental run.

A 1-ft. strip of millimeter paper centered at the hole for the syringe was pasted lengthwise on the back of the glass tube. This strip was made waterproof by covering it with plastic tape. Its purpose was to serve as a reference for the measurement of displacements.

The pressure pulse was generated by the piston and cylinder assembly shown in Figure 2. Bore and stroke were both 1-13/16 in. The assembly was connected by a vee-belt via stepped pulleys to a speed reducer with a range of 400-0-400 rev./min. when driven at 1,750 rev./min. The speed reducer was mounted on a ⅛ h.p., 1,750 rev./min. electric motor. Speed of the pulse generator was thus variable in steps from 0.041 to 6.98 cycles/sec., depending on the setting of the speed reducer and the arrangement of stepped pulleys used. Amplitude of the pressure pulse was adjusted by the pressure control valves indicated in Figure 1.

Fluids Used

A number of viscoelastic polymer solutions, both water based and organic based, were made up to the desired concentrations by the gravimetric method. In addition, a Newtonian oil was procured to serve as a standard test liquid.

Table 1. Fluids Used in Experiments

Number	Solute and source	Solvent	Concentration (% by weight)	Age at time of use (days)
1.	7H CMC*, Hercules Powder Co.	Water	1.0	12
2.	7H CMC*, Hercules Powder Co.	Water	1.0	57
3.	7H CMC*, Hercules Powder Co.	Water	0.75	57
4.	7H CMC*, Hercules Powder Co.	Water	0.50	57
5.	Lucite 41 polymethyl methacrylate, E. I. DuPont de Nemours & Co.	*n*-butyl acetate	13.0	27
6.	Vistanex L-100 Polyisobutylene, Enjay Laboratories	Tetralin	8.0	87
7.	Oronite Polybutene 24, California Chemical Co.	—	—	—

* Sodium carboxymethyl cellulose.

Water-based polymer solutions were made up by sprinkling the dried powder onto the surface of water in a Waring blender. A preservative (0.02% sodium pentachlorophenoate) was added to the aqueous solutions since they are subject to contamination and subsequent degradation by air-borne microbial flora. Polymer solutions in organic solvents were made up by rotating jars containing solvent and weighed amount of solid in a ball mill until all solid had dissolved (12 to 22 days). No preservative was added in these cases. Fluids were used after varying lengths of time, thus yielding some information on the effect of age on rheological properties. Table 1 gives a summary of the materials used.

Procedure

About ½ gal. of fluid was placed in the glass tube and reservoir. The level in the reservoir was about 1 in. above its bottom. Constant temperature water was then circulated through the trough and 3 hr. allowed for temperature equilibration of the test liquid. All experiments were conducted at 30°C.

During the period of temperature equilibration, the charcoal marker was inserted in the test fluid as described above.

The Visicorder, a 1-sec. sweep stop watch, and the center of the test section with the marker were arranged as indicated in Figure 1 so that the reading of the Visicorder, the time, and the displacement profile could all be photographed on the same film. This arrangement was evenly lighted by two 150-w. spot lamps placed at an angle to avoid glare. A 16-mm. movie camera fitted with a close-up lens was used for photography.

When temperature equilibration had been attained, the compressor was started at a preselected frequency and the amplitude of the displacement pulse adjusted to about 1 cm. (at the center line). Five or six cycles were allowed to pass in order for transients to decay; the camera was then started and the displacement followed for about 10 cycles. The camera speed was 12, 18, 32, 48, or 64 nominal frames/sec., depending on the frequency of the compressor.

RESULTS

The variables to be determined from the films were the displacement at the center line (with respect to some arbitrary datum) and the pressure at the position of the transducer. Both of these can be read from the filmed records of the experiments as functions of time, since the time recorded by the stop watch also shows on the film. Data were read from the films with a microreader and were taken at various frames throughout 3 to 6 cycles of the pressure wave.

Figure 3 shows a typical set of data as read from the films. Circles represent experimental values of displacement and pressure; the lines are sine waves having appropriate amplitude, frequency, and phase. One sees that the pressure pulse deviates somewhat from a sine curve, particularly near zero pressure difference. This contributes to errors in values of rheological constants determined from the data; it is probably not more serious than other sources of error, such as neglect of end effects.

Dimensionless Amplitude Ratio

One can show that the amplitude of the displacement pulse at $r = 0$ for a Newtonian fluid, under conditions where inertial forces are small relative to other forces acting (that is at low frequency), is $R^2P/4\eta\omega$. Hence, the ratio $4\eta\omega\Delta/R^2P$ is dimensionless and in accordance with Equation (20) approaches value unity as the frequency goes to zero for all fluid materials. Thus, it will be convenient to plot $4\eta\omega\Delta/R^2P$ as a function of frequency; in the following, the former quantity is referred to as the dimensionless amplitude ratio.

The amplitude Δ may be obtained by averaging the peak heights in graphs such as Figure 3; Figure 4 is a plot of the dimensionless amplitude ratio so obtained for test fluid No. 1. Data for large amplitudes (amplitudes about twice as large as those called small) superimpose on data for small amplitudes. Hence, it is concluded that the linear equations used in the theory are applicable.

As mentioned above, earlier experiments with simple harmonic deformation in the concentric cylinder device were rather insensitive to the nature of the fluid, since, among other things, the amplitude-frequency relation exhibits a maximum near the natural frequency for all materials. There is no question of a natural frequency in the present experiments, and the occurrence of a maximum in the amplitude-frequency relation is a clear indication of the presence of fluid elasticity.

Thus, Figure 4, for the viscoelastic fluid No. 1, should be compared with Figure 5, for the purely viscous fluid No. 7. One sees that theory and experiment agree in asserting that the dimensionless amplitude ratio for fluid No. 7 should be constant at all frequencies studied.

The fact that $\lim_{\omega \to 0} (4\eta\omega\Delta/R^2P) = 1$ can be used to calculate the viscosity from the experimental data. One simply finds the asymptote of a plot of $\omega\Delta/P$ as the frequency goes to zero; this is then equal to $R^2/4\eta$. This method was used for the determination of fluid viscosity.

Finally, the matter of fitting a curve to data such as those of Figure 4 arises. The authors' first impulse was to follow the method suggested earlier (9) and fit the three constant model (η, λ_o, μ_o) to the data. This can be done, and a good fit can in fact be obtained. For instance, in Figure 4 the constants for the dashed line are $\eta = 16.0$ poise, $\lambda_o = 0.30$ sec., and $\mu_o = 0.075$ sec. A better fit could possibly be obtained by modifying these constants slightly.

However, when the three-constant model was applied to other data taken in the experiments (see below), it was found that the model was inadequate in certain respects. Hence, one sees that it may be quite misleading to draw conclusions from a single set of data, such as the amplitude-frequency relation.

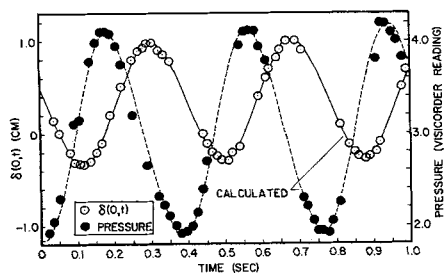

Fig. 3. Displacement and pressure wave for 1% CMC solution at 16.63 sec.$^{-1}$ frequency. The calculated curves are sine waves having the proper amplitude, frequency, and phase.

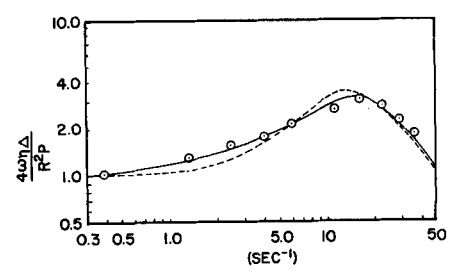

Fig. 4. Dimensionless amplitude ratio for solution No. 1. Solid line—calculated for five-constant model, dashed line—calculated for three-constant model.

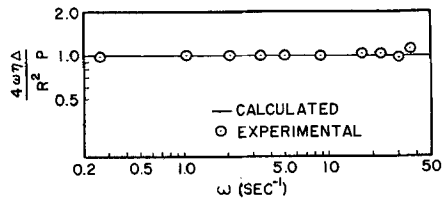

Fig. 5. Dimensionless amplitude ratio for fluid No. 7. Solid line calculated with $\eta = 145$ poise.

The Phase Lag

The phase lag at the center line ϕ may be found by measuring and averaging over several cycles the distance between wave peaks in graphs such as Figure 3. A typical plot of data so obtained is shown in Figure 6. The phase lag may also be calculated for various models, and these are also shown in Figure 6. One sees that as with the amplitude ratio, the three-constant model gives a good fit of the data. The same sets of constants were used for both amplitude ratio and phase lag calculations, of course.

Figure 7 gives experimental and calculated values of the phase lag for the purely viscous material, fluid No. 7. The value $\phi = \pi/2$ is the limiting value of the lag for all fluid materials as the frequency goes to zero. The cause of the deviation of data from the lines at the smallest frequencies is not known. Deviation also occurred with some of the other fluids studied, see, for example, Figure 6.

The Fourier Transform of the Relaxation Function

It can be shown that the Fourier transform of the relaxation function is the same as the complex viscosity used by Williams and Bird (*15*) and many others. Hence, the authors call $\Psi(\omega)$ the *complex viscosity*. The parts $\gamma(\omega)$ and $\zeta(\omega)$ of the complex viscosity, defined by Equation (18), can be found from experimental data by the procedure outlined under theory. Figure 8 is a plot of $\gamma(\omega)$ and $\zeta(\omega)$ for solution No. 1.

Values of $\gamma(\omega)$ and $\zeta(\omega)$ can also be calculated for the operator equation model [Equation (19)]. In particular, for the three-constant model, one finds that

$$\gamma(\omega) = \eta \frac{1 + \lambda_o\mu_o\omega^2}{1 + \lambda_o^2\omega^2} \qquad (23a)$$

$$\zeta(\omega) = \eta \frac{(\lambda_o - \mu_o)\omega}{1 + \lambda_o^2\omega^2} \qquad (24a)$$

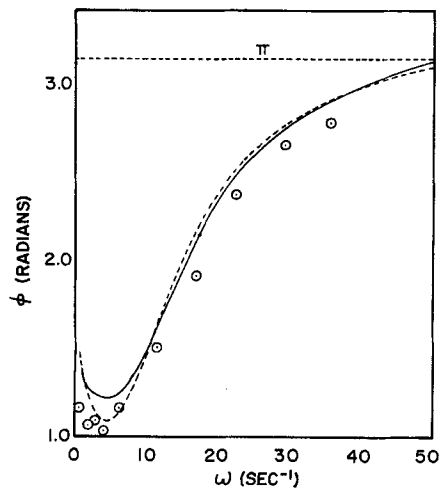

Fig. 6. Phase lag for solution No. 1. Solid line—calculated with five-constant model, dashed line—calculated with three-constant model.

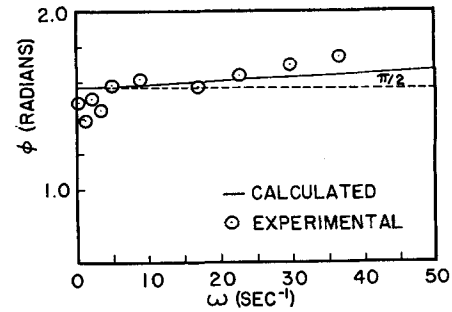

Fig. 7. Phase lag for fluid No. 7. Line calculated with $\eta = 145$ poise.

whereas for the five-constant model

$$\gamma(\omega) = \eta \frac{1 + (\lambda_o\mu_o - \lambda_1 - \mu_1)\omega^2 + \lambda_1\mu_1\omega^4}{1 + (\lambda_o^2 - 2\lambda_1)\omega^2 + \lambda_1^2\omega^4} \qquad (23b)$$

$$\zeta(\omega) = \eta \frac{[(\lambda_o - \mu_o) - (\lambda_o\mu_1 - \lambda_1\mu_o)\omega^2]\omega}{1 + (\lambda_o^2 - 2\lambda_1)\omega^2 + \lambda_1^2\omega^4} \qquad (24b)$$

These equations show, among other things, that if the three-constant model is adequate, then $\eta\omega/\zeta(\omega)$ should be a linear function of ω^2. This was not found to be the case, except perhaps at the very lowest frequencies used. The indicated plot of data on fluid No. 1 is shown in Figure 9.

Hence, the five-constant model was tried in the hope that it would provide a better fit of the data. The viscosity η was found from the low-frequency asymptote of the dimensionless amplitude ratio plot, as explained previously The other constants (λ_0, λ_1, μ_0, μ_1) were determined by fitting Equations (23*b*) and (24*b*) to the complex viscosity data. For details see Vela (*13*). The same procedure was used in the case of the three-constant model. Constants so determined do not represent best values, of course, since a rigorous procedure such as least squares was not used. The reason for not adopting a rigorous procedure was simply that each set of constants must fit several sets of data (dimensionless amplitude ratio and phase lag as well as complex viscosity data).

Constants determined by the foregoing procedure, for both the three- and five-constant models, are given in Table 2 for all fluids studied.

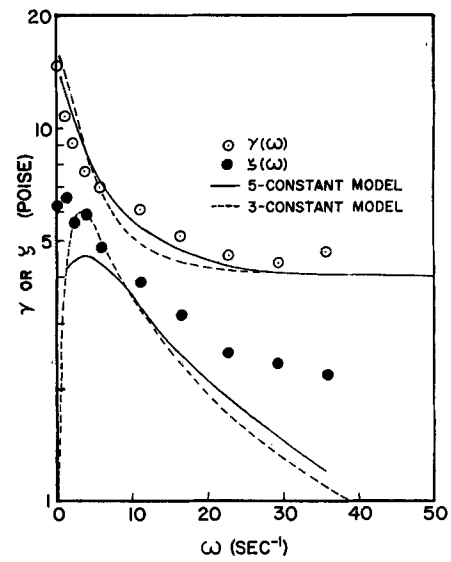

Fig. 8. Parts of the complex viscosity for fluid No. 1. Solid lines—calculated with five-constant model, dashed lines—calculated with three-constant model.

TABLE 2. RHEOLOGICAL PROPERTIES OF FLUIDS*

Fluid no.	ρ, (g./cc.)†	η, (poise)	For the three-constant model λ_o, (sec.)	For the three-constant model μ_o, (sec.)	For the five-constant model λ_o, (sec.)	For the five-constant model μ_o, (sec.)	For the five-constant model λ_1, (sec.^{2})	For the five-constant model μ_1, (sec.^{2})
1	1.002	16.0	0.30	0.075	1.13	0.74	0.17	0.041
2	1.000	6.1	0.12	0.061	0.44	0.31	0.015	0.0053
3	1.000	2.74	0.050	0.025	0.038	0.32	0.010	0.0032
4	1.000	2.40	**	—	—	—	—	—
5	0.903	78	0.055	0.020	0.25	0.23	0.0084	0.0037
6	0.956	105	0.195	0.10	0.45	0.36	0.024	0.010
7	0.891	145	—	—	—	—	—	—

* All data at 30°C.
† Densities were determined with a pycnometer.
** This fluid did not deviate markedly from Newtonian behavior.

The fit of the five-constant model to the dimensionless amplitude ratio data, the phase lag data, and the complex viscosity data is shown in Figures 4, 6, and 8 for fluid No. 1. The fit is as good as that obtained with the three-constant model, but it is not better.

The prediction of the five-constant model for the $\eta\omega/\zeta$ vs. ω^2 plot is shown in Figure 9. There is only slight improvement over the three-constant model's prediction. No doubt an excellent fit of data could be obtained here with the five-constant model, but then the other data might not be fitted as well.

Hence, Occam's razor may be applied, and it leads to the conclusion that the five-constant model is not justified by the existing data.

DISCUSSION AND CONCLUSIONS

One of the principal hypotheses upon which the theory of the experiments is based is that response of the material studied is linear. This was tested by taking data at different amplitudes of oscillation, over the whole range of frequencies studied. Since amplitude ratios and phase lags were independent of amplitude, within the limits of experimental error, it was concluded that the hypothesis of linearity was applicable.

The experiment was found to distinguish sharply between elastic and purely viscous materials, even without extensive analysis of experimental data. That is, if the amplitude ratio-frequency plot shows a maximum, the presence of elasticity is indicated.

The three-constant model correctly predicts trends of all quantities measured. In fact, a fairly good quantitative fit of data is obtained in all cases save that of the part

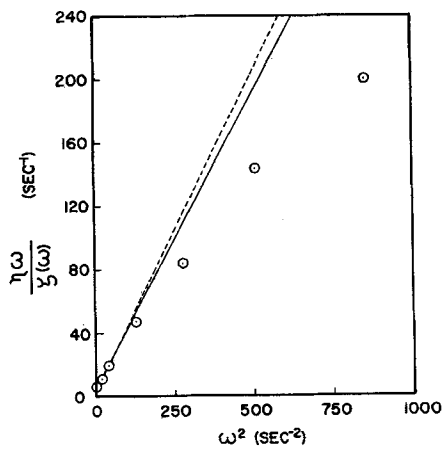

Fig. 9. Plot of $\eta\omega/\zeta(\omega)$ vs. ω^2 for solution No. 1. Solid line—calculated with five-constant model, dashed line—calculated with three-constant model.

$\zeta(\omega)$ of the complex viscosity. The ability of this model to correlate results would be more strongly demonstrated if there were space to include plots of data for all fluids used. The shapes of curves vary greatly from fluid to fluid, and the model faithfully follows the trends.

The effects of age and polymer concentration on the constants of the model are qualitatively what would be expected. In CMC, there is apparently some breakdown with time of the molecular structure causing elastic effects; apparently, this is not due to microbial action, since the authors tried to make the CMC solutions unsuited for microbial habitation by the addition of preservative. Thus, the effect may be due to a slow depolymerization reaction. Further studies on the effect of polymer concentration and molecular weight, the effect of temperature, etc., might prove very useful in the development of molecular theories of viscoelasticity.

One sees from Table 2 that the time constants (λ_o, μ_o) of the organic-based solutions (Nos. 5 and 6) are generally smaller than those for the 1% CMC solutions. On the other hand, the viscosity is higher for the organic-based solutions. This conclusion was also reached by Kapoor et al. (7) on the basis of their recoil experiments with similar fluids (but not at the same concentrations or temperature, unfortunately).

It has been shown that the simple harmonic deformation experiment does not establish the uniqueness of the model used for analyzing data. In particular, either the three- or the five-constant model give reasonable fits of all the primary data. Hence, it appears that the next step in the program should be to do two experiments, simple harmonic deformation and recoil, on the same fluids under identical conditions of temperature and past history.

Finally, a study of the normal stress effect could serve as a further (though less sensitive) test of a model, since it is known (4) what the normal stress effect corresponding to a given model should be.

ACKNOWLEDGMENT

Acknowledgment is made to the donors of the Petroleum Research Fund, administered by the American Chemical Society, for support of this research. The authors also wish to thank Professor W. R. Schowalter and their two reviewers for many helpful suggestions and criticisms.

NOTATION

e^{*mn} = rate of strain tensor
g^{ij} = associated metric tensor
Im = imaginary part of quantity following
i = $\sqrt{-1}$
J_o = Bessel function of first kind and zero order
P = amplitude of the pressure gradient, dynes/cc.
p = hydrostatic pressure, dynes/sq. cm.

R = pipe radius, cm.
Re = real part of quantity following
r, θ, z = cylindrical coordinates
S^{ij} = stress tensor
t, t', τ = time, sec.
u = axial speed, cm./sec.
$\mathbf{X}$ = position vector of material point at time t'; components X^1, X^2, X^3
$\mathbf{x}$ = position vector of material point at time t; components x^1, x^2, x^3
α = defined by Equation (13)
γ = defined by Equation (18)
Δ = amplitude of displacement wave at center line, cm.
δ = displacement, cm.
$\delta(t)$ = Dirac delta function
ζ = defined by Equation (18)
η = viscosity, poise
Θ = normal stress coefficient, g./cm.
$\lambda_o, \ldots \mu_o, \ldots$ = constants in operator equation
ρ = density, g./cc.
ϕ = phase lag, rad.
Ψ = complex viscosity, poise
$\psi(t)$ = relaxation function, dynes/sq. cm.
ω = frequency, sec.$^{-1}$

LITERATURE CITED

1. Alfrey, T., Jr., and E. F. Gurnee, "Rheology," Vol. 1, Chap. 11, pp. 387-429, F. R. Eirich, ed., Academic Press, New York (1956).
2. Broer, L. J. F., *Appl. Sci. Res.*, **A6**, 226 (1956-'57).
3. Ferry, J. D., "Viscoelastic Properties of Polymers," Chap. 5, Wiley, New York (1961).
4. Fredrickson, A. G., *Chem. Eng. Sci.*, **17**, 155 (1962).
5. ———, "Principles and Applications of Rheology," pp. 139-144, Prentice-Hall, Englewood Cliffs, New Jersey (1964).
6. Kapoor, N. N., M.S. thesis, Univ. Minnesota, Minneapolis, Minnesota (1964).
7. ———, E. A. Brumm, and A. G. Fredrickson, in press.
8. Oldroyd, J. G., *Proc. Roy. Soc. (London)*, **A200**, 523 (1950).
9. ———, *Quart. J. Mech. Appl. Math.*, **4**, 271 (1951).
10. ———, D. J. Strawbridge, and B. A. Toms, *Proc. Phys. Soc.*, **B64**, 44 (1951).
11. Toms, B. A., *Rheologica Acta*, **1**, 137 (1958).
12. ———, and D. J. Strawbridge, *Trans. Faraday Soc.*, **49**, 1225 (1953).
13. Vela, S., Ph.D. thesis, Univ. Minnesota, Minneapolis, Minnesota (1964).
14. Walters, K., *Quart. J. Mech. Appl. Math.*, **13**, 444 (1964).
15. Williams, M. C., and R. B. Bird, *Ind. Eng. Chem. Fundamentals*, **3**, 42 (1964).

Manuscript received July 31, 1964; revision received November 9, 1964; paper accepted November 11, 1964.

Film Instabilities in Two-Phase Flows

SIMON OSTRACH and ALFRED KOESTEL

Case Institute of Technology, Cleveland, Ohio

The major types of instabilities which can alter a given two-phase flow pattern or lead to the breakup of a liquid film are delineated, and their physical mechanisms are discussed. Existing stability criteria are correlated to these basic types, and their application and limitations with respect to actual problems are indicated. Basic areas requiring further study are outlined.

A criterion for determining the breakup length of a liquid film is developed which gives an indication of whether a given instability will lead to low frequency and high amplitude pressure and inventory pulsations. Such phenomena may be undesirable.

Two new aspects of importance to the problem of film instability are introduced which have not been previously studied. These are rotation of the fluids and large disturbances in the flow. Their possible influence on the problem is discussed.

Considerable work has been done to study the motion of liquid films that are driven by gas or vapor flows. A good deal of this work was done in connection with film cooling of rocket nozzles, and some has been done in relation to the design and operation of boilers and condensers. It has been found qualitatively that after some length of flow the vapor-liquid interface becomes wavy, and ultimately the liquid waves either are broken up so that liquid is entrained in the vapor or, in tube flow, the liquid film waves sometimes become so large that they essentially join together from opposite sides and form liquid plugs. This sort of behavior changes the basic flow with resulting changes in the pressure drop and heat transfer and can also lead to other undesirable phenomena in tube flows such as pressure and inventory oscillations.

Accordingly a great deal of effort has been exerted to determine the conditions under which the interfacial waviness occurs so that the various associated flow regimes (such as fog) can be identified and objectionable phenomena avoided. Unfortunately, no general stability criteria for two-phase flows with heat and mass transfer have been determined to date. What do exist are criteria that were either empirically established (and, hence, apply only to a specific configuration, fluid, and restricted range of operating conditions) or that were derived on the basis of adiabatic flows with no mass transfer between the phases. Furthermore, even these criteria apply only to a few of the various types of instabilities possible in an

Alfred Koestel is with Thompson Ramo Wooldridge, Inc., Cleveland, Ohio.